Supramolecular Chemistry
Publication details, including instructions for authors and subscription information:
http://www.informaworld.com/smpp/title~content=t713649759

Metal-Organic Coordination Networks of Ferric Wheels, their Surface-supported Supramolecular Architectures and STM/STS Imaging

Ayuk M. Ako[a]; Harald Maid[a]; Stefan Sperner[a]; Syeda HUMA H. Zaidi[a]; Rolf W. Saalfrank[a]; Mohammad S. Alam[b]; Paul Müller[b]; Frank W. Heinemann[c]
[a] Institut für Organische Chemie, Universität Erlangen-Nürnberg, Erlangen, Germany [b] Physikalisches Institut III, Universität Erlangen-Nürnberg, Erlangen, Germany [c] Institut für Anorganische Chemie, Universität Erlangen-Nürnberg, Erlangen, Germany

To cite this Article Ako, Ayuk M. , Maid, Harald , Sperner, Stefan , Zaidi, Syeda HUMA H. , Saalfrank, Rolf W. , Alam, Mohammad S. , Müller, Paul and Heinemann, Frank W.(2005) 'Metal-Organic Coordination Networks of Ferric Wheels, their Surface-supported Supramolecular Architectures and STM/STS Imaging', Supramolecular Chemistry, 17: 4, 315 — 321

To link to this Article: DOI: 10.1080/10610270500114632

URL: http://dx.doi.org/10.1080/10610270500114632

Supramolecular Chemistry, June 2005 VOL. 17 (4), pp. 315–321

Metal–Organic Coordination Networks of Ferric Wheels, their Surface-supported Supramolecular Architectures and STM/STS Imaging

AYUK M. AKO[a], HARALD MAID[a], STEFAN SPERNER[a], SYEDA HUMA H. ZAIDI[a], ROLF W. SAALFRANK[a,*], MOHAMMAD S. ALAM[b], PAUL MÜLLER[b] and FRANK W. HEINEMANN[c]

[a]*Institut für Organische Chemie, Universität Erlangen-Nürnberg, Henkestr. 42, 91054 Erlangen, Germany;* [b]*Physikalisches Institut III, Universität Erlangen-Nürnberg, Erwin-Rommel-Str. 1, 91058 Erlangen, Germany;* [c]*Institut für Anorganische Chemie, Universität Erlangen-Nürnberg, Egerlandstr. 1, 91058 Erlangen, Germany*

Received (in Southampton, UK) 26 January 2005; Accepted February 2005

Six-membered ferric wheels $[Fe_6Cl_6(L^2)_6]$ were generated from the corresponding *N*-alkylsubstituted diethanolamines (H_2L^2) {L^2 = [®—$N(CH_2CH_2O)_2]^{2-}$; ® = Me—$[CH_2—]_{17}$ (3d); Me—$[CH_2—]_{19}$ (3e)}, calcium hydride and iron(III) chloride. Compound 3d was characterized by X-ray crystal structure analysis. The lipophilic tails of 3d interdigitate to create strands that, by lateral van der Waals interactions, pack to form 2D layers. The stacking of these sheets creates the final 3D architecture of the crystal. An elementary structure formation process of complex molecule 3d on highly oriented pyrolytic graphite (HOPG) was studied. Using scanning tunneling microscopy (STM) under ambient conditions, we succeeded in combining high-resolution topography mapping with simultaneous current–voltage characteristics (scanning tunneling spectroscopy, STS) measurements on single molecules deposited on HOPG surfaces. One of the most interesting results is that the location of the individual metal ions in their organic matrix is directly addressable by STS.

Keywords: Supramolecular coordination chemistry; Self-assembly; Iron wheels on graphite; X-ray structure; STM images

INTRODUCTION

Over the past years, considerable progress has been made towards the predictability of ordered supramolecular assemblies on the basis of coordinative metal–ligand bonds [1–24]. A particular symmetrical class comprises the so-called ferric wheels with 6, 8, 10, 12 and even 18 iron(III) ions [25–41]. Recently, we reported the template-mediated self-assembly of six- and eight-membered iron coronates $\{Na \subset [Fe_6(L^1)_6]\}^+$ (**1**) and $\{Cs \subset [Fe_8(L^1)_8]\}^+$ (**2**) [42–46]. They were prepared from *tri*ethanolamine (H_3L^1) with iron(III) chloride, sodium hydride or cesium carbonate (Scheme 1). A common feature of **1** and **2** is that the oxygen donors of one of the ethanolate arms function solely as ligands for the coordinative saturation of the iron centers and for charge compensation, whereas the ethanolato μ_2-O donors are structure determining; they are linkers, necessary for the ring formation. Reaction of *N*-substituted *di*ethanolamines (H_2L^2) {L^2 = [®—$N(CH_2CH_2O)_2]^{2-}$} with calcium hydride and iron(III) chloride yielded the unoccupied neutral iron coronands $[Fe_6Cl_6(L^2)_6]$ (**3**) [47]. As in **1** and **2**, the μ_2-O donors of the methyldiethanolamine ligands in **3a** are structure determining. Completion of the octahedral coordination sphere at iron and charge compensation are achieved by the chloride co-ligands (Scheme 1). This new synthesis of six-membered ferric wheels was applied to the convergent synthesis of metallo-dendrimers [48–51]. Variable-temperature NMR spectroscopy carried out on a diamagnetic indium analog revealed that these species are not rigid but instead undergo nondissociative topomerization processes [50].

An interesting feature of oligonuclear assemblies is their readiness to frame compartments and 3D networks with discrete channels and pores [52–64]. Principally, all the six-membered ferric wheels $[Fe_6Cl_6(L^2)_6]$ (**3**) are isostructural; however, there are fundamental differences concerning their crystal packing [51]. For example, all the disk-like clusters of **3a–c** (space group $R\bar{3}$) are arranged in parallel and

---

*Corresponding author. Tel.: +49-9131-852-2554. Fax: +49-9131-852-1165. E-mail: saalfrank@chemie.uni-erlangen.de

ISSN 1061-0278 print/ISSN 1029-0478 online
DOI: 10.1080/10610270500114632

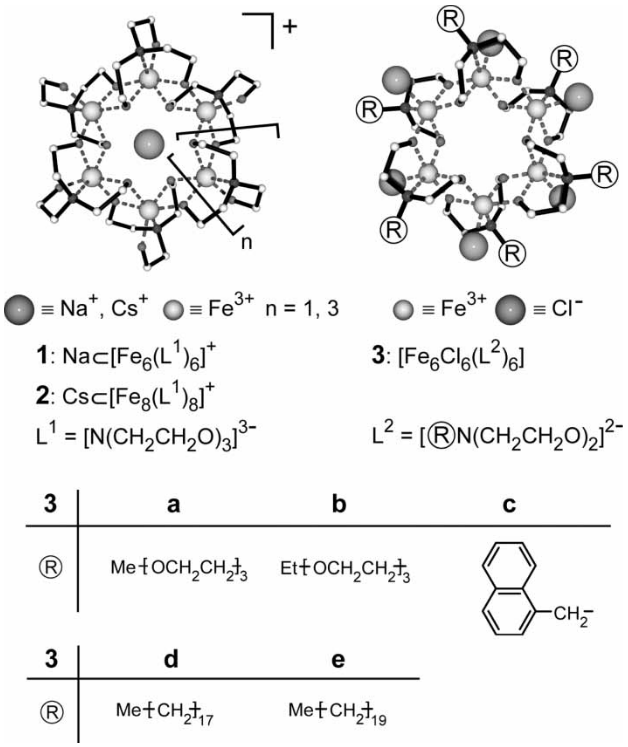

SCHEME 1 Schematic representation of the metalla-coronates **1** and **2** and metalla-coronands **3**.

are piled up in cylindrical columns, with all the iron centers superimposed. Each column is surrounded by six parallel columns that are alternately dislocated by 1/3 *c* and 2/3 *c* against the central column (Fig. 1).

An additional interesting feature of some ferric wheels is their readiness to create various substructures, depending on the nature of their side arms. For instance, van der Waals interactions cause the side arms of **3b** (Fig. 2) to interlock and give rise to the formation of compartments occupied by chloroform. An especially remarkable example of crystal packing leading to porous frameworks is caused by 3D $\pi-\pi$ stacking of the naphthyl groups of the side arms of the ferric wheels **3c** (Fig. 2) [51].

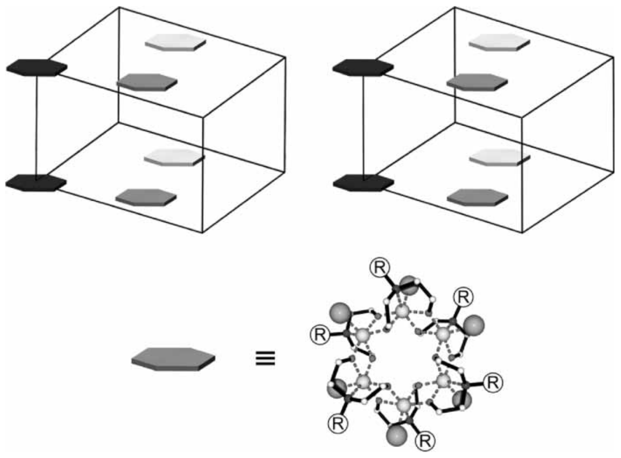

FIGURE 1 Stereopresentation of the crystal packing of **3a**–**c**.

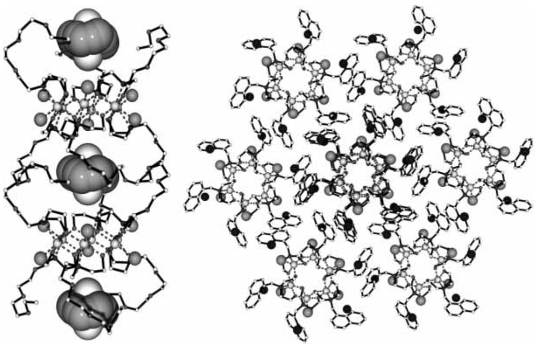

FIGURE 2 Left: Presentation of the columnar crystal packing of **3b**, highlighting the compartments with encapsulated chloroform. Right: Crystal packing of **3c**, highlighting the $\pi-\pi$ interactions together with trapped water.

The absorption of supramolecules on surfaces has recently been the subject of intense investigation because surface-oriented supramolecular structures are the basis for the construction of new functional materials and nanoobjects in a bottom-up strategy [65,66]. Certain complex molecules are considered good candidates as basic building blocks for molecular electronics and nanomechanical devices [67]. Impressive first examples are molecular switches and nanowires. A more recent objective is the controlled assembling of supramolecular metal complexes on surfaces. Scanning tunneling microscopy (STM) has proved to be a powerful tool to study various surfaces at the atomic and molecular level. Although STM measurements reveal electronic structure information, separating the contributions of electronic and geometrical characteristics is not straightforward. Electronic structure information is more directly accessible from scanning tunneling spectroscopy (STS). In the present work we present the 2D structure of ring-shaped **3d** and its STM/STS measurements on highly oriented pyrolytic graphite (HOPG).

EXPERIMENTAL

All reactions were carried out under an atmosphere of dry nitrogen. All solvents were purified and dried according to standard literature procedures [68]. Commercially available starting materials were purchased from Aldrich or Fluka and were used as received. ^1H and ^{13}C NMR spectra were recorded on JEOL EX 400 and GX 400 spectrometers at 400 and 100.5 MHz, respectively. Solvent signals were used as internal standard: $CDCl_3$ (^1H, 7.24 ppm; ^{13}C, 77.0 ppm). IR spectra were recorded on a Bruker IFS25 spectrometer. Mass spectra were recorded on a Varian MAT CH-48 (EIMS, 70 eV) spectrometer or on a Micromass ZabSpec-E (8 kV) spectrometer in the fast atom bombardment (FAB) mode with 3-nitrobenzyl alcohol (3-NBA) as the matrix.

Elemental analyses were performed on a EA1110 CHNS-Microautomat. Melting points were measured with a DSC 821 Mettler Toledo calorimeter.

Ligand Syntheses (H_2L^2)

The ligands were prepared as described previously for similar compounds by heating the corresponding bromides, diethanolamine and Na_2CO_3 in CH_3CN for 48 h [51].

N-Octadecyldiethanolamine (® = $Me{-}[CH_2{-}]_{17}$)

Starting material: 1-Bromooctadecane (5 g). Yield: 3.90 g (73%), pale yellow oil that solidified on standing. IR (neat) : $\tilde{\nu} = 3371$, 2845, 1465, 1143, 1065 cm^{-1}. ^1H NMR (400 MHz, $CDCl_3$): $\delta = 3.60$ (t, $J = 5.4$ Hz, 4H, 2 $CH_2{-}OH$), 3.11 (br s, 2H, 2 OH), 2.72 (t, $J = 5.4$ Hz, 4H, 2 $N{-}CH_2$), 1.22 (m, 34H, 17 CH_2), 0.91 (t, 3H, CH_3) ppm. ^{13}C NMR (100.5 MHz, $CDCl_3$): $\delta = 59.53$ (2 $CH_2{-}OH$), 56.08 (2 $N{-}CH_2$), 32.83, 32.92, 29.69 (overlapping signals), 29.55, 29.43, 29.35, 28.17, 27.35, 26.92, 22.67, 22.62 (17 CH_2), 14.11 (CH_3) ppm. MS (EI, 70 eV): $m/z\,(\%) = 356$ (5) $[M]^+$, 326 (90) $[M{-}CH_2O]^+$, 118 (65) $[M{-}CH_2{-}N(CH_2CH_2OH)_2]^+$. Anal. Calcd (%) for $C_{22}H_{47}NO_2$ (357.63): C, 73.89; H, 13.25; N, 3.92. Found: C, 73.87; H, 13.57; N, 3.70.

N-Ecosyldiethanolamine (® = $Me{-}[CH_2{-}]_{19}$)

Starting material: 1-Ecosylbromide (5 g). Yield: 3.80 g (71%), colorless oil that solidified on standing. IR (neat) : $\tilde{\nu} = 3355$, 2961, 2845, 1620, 1300, 1060, 750 cm^{-1}. ^1H NMR (400 MHz, $CDCl_3$): $\delta = 3.61$ (t, $J = 5.3$ Hz, 4H, 2 $CH_2{-}OH$), 3.06 (br s, 2H, 2 OH), 2.74 (t, $J = 5.3$ Hz, 4H, 2 $N{-}CH_2$), 1.56 (m, 38H, 19 CH_2), 0.91 (t, 3H, CH_3) ppm. ^{13}C NMR (100.5 MHz, $CDCl_3$): $\delta = 59.58$ (2 $CH_2{-}OH$), 56.06 (2 $N{-}CH_2$), 54.78 ($CH_2{-}N$), 31.91, 29.69, 29.64, 29.62, 29.56 (overlapping signals), 29.35, 27.36, 27.01, (18 CH_2), 22.68 ($CH_2{-}CH_3$), 14.10 (CH_3) ppm. MS (EI, 70 eV): $m/z\,(\%) = 385$ (5) $[M]^+$, 354 (100) $[M{-}CH_2OH]^+$, 118 (60) $[M{-}CH_2{-}N(CH_2CH_2OH)_2]^+$. Anal. Calcd (%) for $C_{24}H_{51}NO_2$ (385.68): C, 74.74; H, 13.33; N, 3.63. Found: C, 74.71; H, 13.41; N, 3.70.

Complex Syntheses: General Method for $[Fe_6Cl_6(L^2)_6]$ (3d,e)

To a suspension of calcium hydride (253 mg, 6 mmol) in anhydrous THF (75 ml), the corresponding *N*-substituted diethanolamine (H_2L^2) (4 mmol) was added. After the mixture had been stirred for 1 h at 20°C, a solution of anhydrous iron(III) chloride (650 mg, 4 mmol) in anhydrous THF (25 ml) was added dropwise. Stirring was continued at ambient temperature for 48 h, after which the reaction mixture was filtered and the solvent removed *in vacuo*. The yellow residue was dried under vacuum, and crystallized.

$[Fe_6Cl_6(L^2)_6]$ (3d)

Starting material: *N*-Octadecyldiethanolamine (141 mg). Yield: 62 mg (44%) yellow plate-like crystals from dichloromethane and diffusion of diethyl ether. Mp 107–108°C. IR (KBr): $\tilde{\nu} = 3350$, 2923, 2858, 1465, 1080 cm^{-1}. MS (FAB): m/z (%) = 2682 (5) $[Fe_6Cl_6(L^2)_6]^+$, 2644 (10) $[Fe_6Cl_5(L^2)_6]^+$, 1878 (25) $[Fe_5Cl_5(L^2)_4]^+$, 1752 (65) $[Fe_4Cl_3(L^2)_4]^+$, 1269 (100) $[Fe_3Cl(L^2)_3]^+$. Anal. Calcd (%) for $C_{132}H_{270}Cl_6Fe_6N_6O_{12}$ (2681.34): C, 59.13; H, 10.15; N, 3.13. Found: C, 58.95; H, 10.37; N, 2.99.

$[Fe_6Cl_6(L^2)_6]$ (3e)

Starting material: *N*-Ecosyldiethanolamine (144 mg). Yield: 56 mg (37%) yellow microcrystalline platelets from dichloromethane and diffusion of diethyl ether. Mp 108–109°C. (Note the low melting points of both **3d** and **3e**.) IR (KBr): $\tilde{\nu} = 3056$, 2928, 2857, 1466, 1080 cm^{-1}. MS (FAB): m/z (%) = 2813 (45) $[Fe_6Cl_5(L^2)_6]^+$, 2248 (25) $[Fe_4Cl_3(L^2)_5]^+$, 1863 (80) $[Fe_4Cl_3(L^2)_3]^+$, 1353 (100) $[Fe_3Cl(L^2)_3]^+$. Anal. Calcd (%) for $C_{144}H_{294}Cl_6Fe_6N_6O_{12}$ (2849.79): C, 60.69; H, 10.39; N, 2.95. Found: C, 61.07; H, 10.61; N, 2.80.

Single-crystal X-ray Structure Analysis of 3d

Details of crystal data, data collection and refinement are given in Table I. X-ray data were collected on a Nonius KappaCCD area detector using Mo Kα radiation ($\lambda = 0.71073$ Å). A semiempirical absorption correction based on multiple scans was applied ($T_{\min} = 0.838$, $T_{\max} = 1.000$, SADABS [69]). A total of 54 946 reflections were collected, of which 12 750 were independent reflections and 7341 observed reflections [$I > 2\sigma(I)$]. The structure was solved by direct methods and refined with full-matrix least-squares procedures on F^2 using SHELXTL NT 6.12 [69]. All nonhydrogen atoms were refined anistropically. Hydrogen atoms were attached in idealized positions and refined using the riding model; their isotropic displacement parameters were tied to those of the corresponding carrier atoms by a factor of 1.2 or 1.5. A considerable amount of disorder is observed in the structure. The disorder involves some of the atoms on the iron wheel side of two of the aliphatic chains as well as some of the atoms comprising the iron wheel. This results in two orientations of the molecule so that the l.s. plane calculated through the six iron atoms of orientation part 1 (with 82.4(3)% occupancy) is slightly tilted against the corresponding l.s. plane of the six iron centers of the minor orientation (part 2,

TABLE I Crystallographic data, data collection and refinement parameters for **3d**

Empirical formula	$C_{132}H_{270}Cl_6Fe_6N_6O_{12}$
Formula weight	2681.34 g mol^{-1}
Temperature	100(2) K
Wavelength	0.71073 Å
Crystal system	Triclinic
Space group	$P\bar{1}$
Unit cell dimensions	
$a = 11.8461(6)$ Å	$\alpha = 76.811(9)°$
$b = 12.990(2)$ Å	$\beta = 88.165(5)°$
$c = 24.406(2)$ Å	$\gamma = 85.320(7)°$
Volume, Z	3644.0(7) Å^3, 1
Density (calculated)	1.222 Mg m^{-3}
Absorption coefficient	0.746 mm^{-1}
$F(000)$	1458
Crystal size	0.34 × 0.30 × 0.05 mm
Θ range for data collection	3.15–25.03°
Index ranges	$-13 \leq h \leq 14$, $-15 \leq k \leq 15$, $-29 \leq l \leq 29$
Reflections collected	54,946
Independent reflections	12,750 [R(int) = 0.0749]
Data/restraints/parameters	12,750/332/917
Goodness-of-fit on F^2 (all data)	1.043
Final R indices [$I > 2\sigma(I)$]	$R1 = 0.0777$, $wR2 = 0.1753$
R indices (all data)	$R1 = 0.1515$, $wR2 = 0.2105$
Largest diff. peak and hole	0.948 and -0.848 e Å^{-3}

17.6(3)% occupancy) by an angle of 9.7°. Further details on the treatment of this disorder can be found in the deposited material (in CIF form). Crystallographic data (excluding structure factors) for structure **3d** reported in this paper have been deposited with the Cambridge Crystallographic Data Centre as supplementary publication no. CCDC 261471. Copies of the data can be obtained free of charge at www.ccdc.cam.ac.uk/products/csd/request/ (or from the CCDC, 12 Union Road, Cambridge CB2 1EZ, UK; fax: (+44)1223-336-033; or deposit@ccdc.cam.ac.uk).

STM Experiments

STM measurements were carried out at ambient conditions using a home-built, low-drift microscope equipped with a commercial low-current RHK1000 control system. Before imaging, the sample was dissolved in dichloromethane/acetone (30/70) and a drop of 10^{-9} M solution was applied to a freshly cleaved surface of HOPG. Before placing the drop, the surface had already been scanned by STM, which allowed monoatomic resolution of the graphite structure. Different settings for the tunneling current and the bias voltage were used, ranging from 5 to 50 pA and ±50 to ±100 mV, respectively. The scan frequency was varied between 2 and 5 Hz. Resolution was 256 × 256 points for topography, and 128 × 128 in the current imaging tunneling spectroscopy (CITS) measurements. The tip was prepared by cutting a 0.25-mm diameter platinum-iridium (90/10) wire at room temperature.

RESULTS AND DISCUSSION

We discuss here the synthesis, metal-organic coordination networks (MOCNs) [70,71] and STM/STS topography images of chains of **3d** on HOPG.

Synthesis of Ferric Wheels 3d,e

The six-membered ferric wheels $[Fe_6Cl_6(L^2)_6]$ (**3d,e**) were generated from the corresponding *N*-alkyl-substituted diethanolamines (H_2L^2), calcium hydride and iron(III) chloride (Scheme 1).

Single-crystal X-ray Structure Analysis of 3d

For an unambiguous characterization, we carried out an X-ray crystallographic structure analysis of **3d** (Tables I and II). Unlike **3a–c** [51], the ferric wheel **3d** has crystallographically imposed C_i molecular symmetry and crystallizes in space group $P\bar{1}$, with all the ferric wheels stacked up in parallel (Fig. 3). The lipophilic tails of **3d** interdigitate to create strands that, by lateral van der Waals interactions, pack to form 2D layers. The stacking of these sheets creates the final 3D architecture of the crystal (Fig. 4). Self-assembly by hydrogen bonding, van der Waals interaction and π–π stacking are widespread binding modes in supramolecular hybrid organic–inorganic 3D networks [51,52].

STM Investigations

Based on the structural features presented by the iron wheel **3d** as revealed by its X-ray structural analysis, complex **3d** was examined on HOPG. The morphology of the monolayers formed upon adsorption on HOPG of ferric wheel **3d**, endowed

TABLE II Selected bond distances (Å) and angles (°) in **3d** with esds in parentheses

Fe(1)—O(2)	1.968(5)	N(1)—C(5)	1.51(1)
Fe(1)—O(3)	1.988(5)	O(1)—C(1)	1.440(7)
Fe(1)—O(1)	2.009(4)	O(2)—C(4)	1.426(8)
Fe(1)—O(6)$^{\#1}$	2.016(4)	C(1)—C(2)	1.520(9)
Fe(1)—N(1)	2.284(7)	C(3)—C(4)	1.52(2)
Fe(1)—Cl(1)	2.324(3)	C(5)—C(6)	1.56(2)
N(1)—C(3)	1.48(1)	C(6)—C(7)	1.51(2)
N(1)—C(2)	1.49(1)		
O(2)—Fe(1)—O(3)	74.8(2)	Cl(1)—Fe(1)—O(6)$^{\#1}$	90.9(2)
O(2)—Fe(1)—O(1)	95.3(2)	Cl(1)—Fe(1)—N(1)	93.1(2)
O(3)—Fe(1)—O(1)	95.6(2)	C(3)—N(1)—C(2)	112.7(6)
O(2)—Fe(1)—O(6)$^{\#1}$	165.8(2)	C(3)—N(1)—C(5)	110.7(7)
O(3)—Fe(1)—O(6)$^{\#1}$	97.2(2)	C(2)—N(1)—C(5)	110.3(6)
O(1)—Fe(1)—O(6)$^{\#1}$	73.5(2)	C(3)—N(1)—Fe(1)	102.8(5)
O(2)—Fe(1)—N(1)	75.9(2)	C(2)—N(1)—Fe(1)	107.1(4)
N(1)—Fe(1)—O(3)	149.8(2)	C(5)—N(1)—Fe(1)	113.0(5)
N(1)—Fe(1)—O(1)	79.9(2)	O(1)—C(1)—C(2)	111.5(5)
N(1)—Fe(1)—O(6)$^{\#1}$	109.7(3)	O(2)—C(4)—C(3)	105.3(6)
Cl(1)—Fe(1)—O(2)	101.9(2)	N(1)—C(2)—C(1)	112.2(5)
Cl(1)—Fe(1)—O(3)	99.9(2)	N(1)—C(3)—C(4)	110.9(7)
Cl(1)—Fe(1)—O(1)	159.3(2)	N(1)—C(5)—C(6)	113.2(7)

$^{\#1}$Symmetry code: $-x+2$, $-y+1$, $-z+1$.

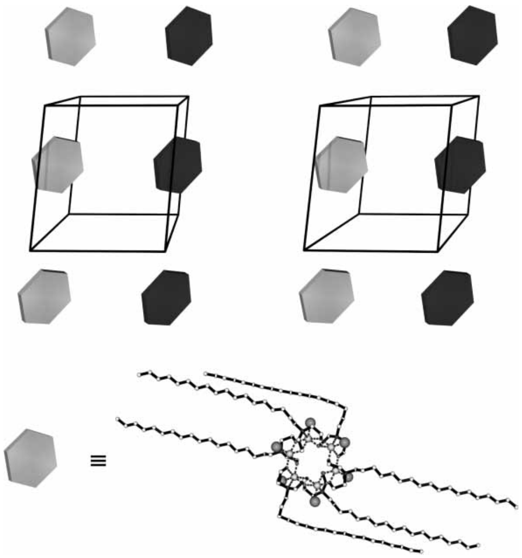

FIGURE 3 Schematic stereopresentation of the packing of the ferric wheels of **3d**.

with extended linear hydrocarbon side-chains, was investigated by *in situ* STM at the liquid-solid interface. The unique shape, packing and known dimensions of **3d** allow for the submolecular analysis of the measured STM images. As the bonding of the molecules to the substrate is weak, diffusion is possible along the surface. This mobility is reduced at defects, e.g. monoatomic graphite steps. Thus, an aggregation of molecules is to be expected, particularly in such places. Fig. 5 depicts the linear interdigitation of the alkyl chains of **3d** to strands, where the molecules are attached to the monoatomic graphite step horizontally. We note that only the molecule centers, that is the rings, are visible (see next section).

CITS Measurements

CITS was developed by Hamers *et al.* [72] to perform STS on a sample surface. At constant tip to sample distance, CITS records current–voltage characteristics at each pixel of the image. Therefore, CITS measures a tunneling spectrum at each pixel of an image and so creates a series of images at different energy levels, which can be understood as maps of the local density of electronic states integrated up to each of those energies. The tip to sample distance is defined by the topography parameters. In our measurements, all potentials are measured against the potential of the tip. The current contrast changes significantly when, at certain bias voltages, new molecular energy levels come into play, thus enhancing the information obtained from topography alone [73,74]. It is a difficult technique to implement successfully, requiring high stability of the tip and sample. The unstable nature of small organic molecules adsorbed to a substrate adds a further difficulty [75]. However, we were able to measure clear CITS images of ferric wheels **3d**. Fig. 6 shows the constant current topography imaging, together with a simultaneously measured CITS image. The topographic image presents a rather washed-out sphere with a diameter of approximately 1.2 nm, which conforms to the outer diameter of the ferric wheel. A current map at −352 mV is also shown, measured simultaneously, and a ring of six peaks is revealed. The ring diameter is approximately

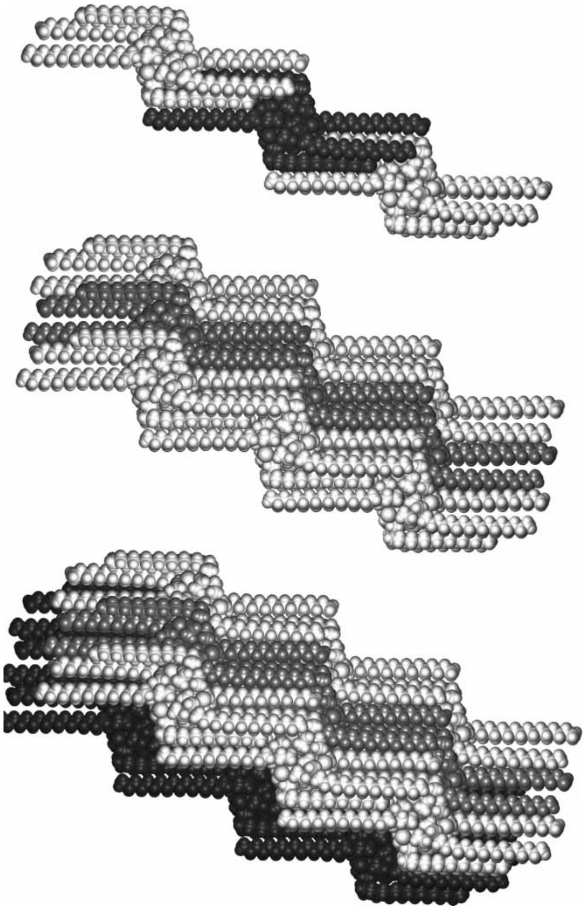

FIGURE 4 Interdigitating alkyl chains, lateral interaction of 1D strands, stacking of 2D layers and final 3D architecture. Midpoint distances (ferric wheels): 27.5 Å along chains, 13.0 Å between strands, 11.9 Å between plains.

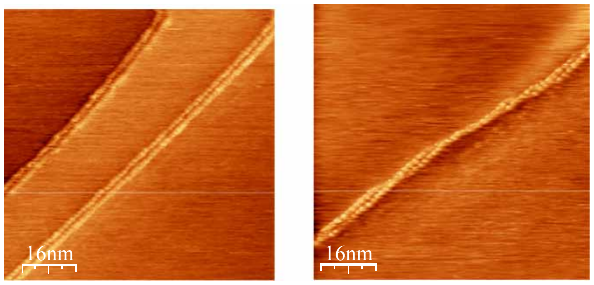

FIGURE 5 Constant current STM topographies of ferric wheels on HOPG showing the formation of double-linear superstructures (left) and double-helical superstructures (right). In both cases the set point voltage is 100 mV and the set point current is 10 pA. The scale is 80 × 80 nm^2 in both pictures.

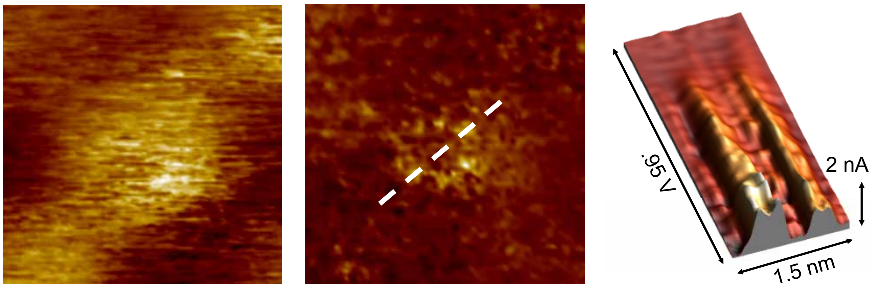

FIGURE 6 STS results of ferric wheels on HOPG. Left: Constant current STM image (topography) recorded simultaneously with the tunneling spectra. The scale is 2.5 × 2.5 nm^2. Set points were 100 mV and 40 pA. Center: Current image of the same area at −352 mV. Right: Current profile along the dashed white line in the middle at voltages between 0, and −0.95 V.

0.65 nm, and the distance between neighboring peaks is roughly 0.3 nm, conforming well to distances between Fe ions of 0.632 nm across the ring, and an average distance of 0.32 nm between neighboring Fe ions, respectively (Scheme 1). The 3D current profile is recorded along the dashed line of the current map, plotted at all voltages between 0 and −0.95 V. The background current arising from the graphite surface has been subtracted. There are two ridges that are approximately 0.6 nm apart. As all distances between the peaks in the CITS pictures conform to the Fe—Fe distances in the molecule, we conclude that we have mapped the local maxima of the density of states arising from the Fe ions.

Despite the high resolution of the STM images shown in Figs. 5 and 6, which allowed the observation of the internal structure of the ferric wheels, the alkyl chains were not observed. We assume that either the energy levels corresponding to the alkyl chains are far away from the Fermi level or the long chains are mobile above the plane of the graphite.

CONCLUSIONS

The six-membered ferric wheels [$Fe_6Cl_6(L^2)_6$] (**3d**,**e**) were generated by self-assembly in a one-pot reaction. X-ray crystallographic studies carried out on **3d** showed that the lipophilic tails of **3d** interdigitate in the crystal to create strands. STM and STS measurements of the ferric wheel **3d** on a HOPG surface at a single molecule level were studied, using a high-resolution home-built scanning tunneling microscope under ambient conditions. The molecules were shown to pack and create strands even at very low coverage. The diameter of the ring structures observed by STM is in agreement with X-ray crystallography data. In addition, we were able to observe the individual metal centers of the ferric wheels by STS. The facility to control the adsorption of such complexes on solid surfaces could provide the feasibility to prepare locally addressable organic storage devices.

Acknowledgements

Financial support by the Deutsche Forschungsgemeinschaft (Sa 276/25-1, SFB 583, SPP 1137, GK 312) and the Fonds der Chemischen Industrie is gratefully acknowledged.

References

[1] Recent reviews: Hof, F.; Craig, S. L.; Nuckolls, C.; Rebek, J. Jr. *Angew. Chem.* **2002**, *114*, 1556.
[2] Recent reviews: *Angew. Chem., Int. Ed. Engl.* **2002**, *41*, 1488.
[3] Recent reviews: Holliday, B. J.; Mirkin, C. A. *Angew. Chem.* **2001**, *113*, 2076.
[4] Recent reviews: *Angew. Chem., Int. Ed. Engl.* **2001**, *40*, 2022.
[5] Recent reviews: Seidel, S. R.; Stang, P. J. *Acc. Chem. Res.* **2002**, *35*, 972.
[6] Recent reviews: Saalfrank, R. W.; Demleitner, B. In *Transition Metals in Supramolecular Chemistry*; Sauvage, J. P., Ed.; Wiley-VCH: Weinheim, 1999; pp 1–51.
[7] Recent reviews: Uller, E.; Demleitner, B.; Bernt, I.; Saalfrank, R. W. In *Structure and Bonding*; Fujita, M., Ed.; Springer: Berlin, 2000; Vol. 96, pp 149–175.
[8] Recent reviews: Caulder, D. L.; Raymond, K. N. *Acc. Chem. Res.* **1999**, *32*, 975.
[9] Recent reviews: Atwood, J. L.; MacGillivray, L. R. *Angew. Chem.* **1999**, *111*, 1080.
[10] Recent reviews: *Angew. Chem., Int. Ed. Engl.* **1999**, *38*, 1018.
[11] Recent reviews: Fujita, M. *Chem. Soc. Rev.* **1998**, *27*, 417.
[12] Recent reviews: Jones, C. J. *Chem. Soc. Rev.* **1998**, *27*, 289.
[13] Recent reviews: Philip, D.; Stoddart, J. F. *Angew. Chem.* **1996**, *108*, 1242.
[14] Recent reviews: *Angew. Chem., Int. Ed. Engl.* **1996**, *35*, 1154.
[15] Recent reviews: Baxter, P. N. W. In *Comprehensive Supramolecular Chemistry*; Lehn, J.-M., Ed.; Pergamon: Oxford, 1996; Vol. 9, pp 165–211.
[16] Recent reviews: Constable, E. C. In *Comprehensive Supramolecular Chemistry*; Lehn, J.-M., Ed.; Pergamon: Oxford, 1996; Vol. 9, pp 213–252.
[17] Recent reviews: Chambron, J.-C.; Dietrich-Buchecker, C.; Sauvage, J.-P. In *Comprehensive Supramolecular Chemistry*; Lehn, J.-M., Ed.; Pergamon: Oxford, 1996; Vol. 9, pp 43–83.
[18] Recent reviews: Piguet, C.; Bernardinelli, G.; Hopfgartner, G. *Chem. Rev.* **1997**, *97*, 2005.
[19] Recent reviews: Saalfrank, R. W.; Demleitner, B.; Löw, N.; Trummer, S.; Kareth, S. *Mol. Cryst. Liq. Cryst.* **2001**, *356*, 71.
[20] Recent reviews: Johnson, D. W.; Raymond, K. N. *Supramol. Chem.* **2001**, *13*, 639.
[21] Recent reviews: Ziegler, M.; Brumaghim, J. L.; Raymond, K. N. *Angew. Chem.* **2000**, *112*, 4285.
[22] Recent reviews: *Angew. Chem. Int. Ed. Engl.* **2000**, *39*, 4119.
[23] Recent reviews: Swiegers, G. F.; Malefetse, T. J. *Coord. Chem. Rev.* **2002**, *225*, 91.
[24] Recent reviews: Ward, M. D.; McCleverty, J. A.; Jeffery, J. C. *Coord. Chem. Rev.* **2001**, *222*, 251.

[25] Oshio, H.; Hoshino, N.; Ito, T.; Nakano, M.; Renz, F.; Gütlich, P. *Angew. Chem.* **2003**, *115*, 233.
[26] *Angew. Chem., Int. Ed. Engl.* **2003**, *42*, 223.
[27] Sydora, O. L.; Woleczanski, P. T.; Lobkovsky, E. B. *Angew. Chem.* **2003**, *115*, 2789.
[28] *Angew. Chem., Int. Ed. Engl.* **2003**, *42*, 2685.
[29] Taft, K. L.; Lippard, S. J. *J. Am. Chem. Soc.* **1990**, *112*, 9629.
[30] Taft, K. L.; Delfs, C. D.; Papaefthymiou, G. C.; Foner, S.; Gatteschi, D.; Lippard, S. J. *J. Am. Chem. Soc.* **1994**, *116*, 823.
[31] Abbati, G. L.; Cornia, A.; Fabretti, A. C.; Malavasi, W.; Schenetti, L.; Caneschi, A.; Gatteschi, D. *Inorg. Chem.* **1997**, *36*, 6443.
[32] Caneschi, A.; Cornia, A.; Lippard, S. J. *Angew. Chem.* **1995**, *107*, 511.
[33] *Angew. Chem., Int. Ed. Engl.* **1995**, *34*, 467.
[34] Caneschi, A.; Cornia, A.; Fabretti, A. C.; Foner, S.; Gatteschi, D.; Grandi, R.; Schenetti, L. *Chem. Eur. J.* **1996**, *2*, 1379.
[35] Pilawa, B.; Desquiotz, R.; Kelmen, M. T.; Weickmeier, M.; Geisselman, A. *J. Magn. Magn. Mater.* **1997**, *177–181*, 748.
[36] Benelli, C.; Parsons, S.; Solan, G. A.; Winpenny, R. E. P. *Angew. Chem.* **1996**, *108*, 1967.
[37] *Angew. Chem., Int. Ed. Engl.* **1996**, *35*, 1825.
[38] Caneschi, A.; Cornia, A.; Fabretti, A. C.; Gatteschi, D. *Angew. Chem.* **1999**, *111*, 1372.
[39] *Angew. Chem., Int. Ed. Engl.* **1999**, *38*, 1295.
[40] Watton, S. P.; Fuhrmann, P.; Pence, L. E.; Caneschi, A.; Cornia, A.; Abbati, G. L.; Lippard, J. S. *Angew. Chem.* **1997**, *109*, 2917.
[41] *Angew. Chem., Int. Ed. Engl.* **1997**, *36*, 2774.
[42] Saalfrank, R. W.; Bernt, I.; Uller, E.; Hampel, F. *Angew. Chem.* **1997**, *109*, 2596.
[43] *Angew. Chem., Int. Ed. Engl.* **1997**, *36*, 2482.
[44] Saalfrank, R. W.; Bernt, I.; Hampel, F. *Angew. Chem.* **2001**, *113*, 1745.
[45] *Angew. Chem., Int. Ed. Engl.* **2001**, *40*, 1700.
[46] Saalfrank, R. W.; Bernt, I.; Hampel, F. *Chem. Eur. J.* **2001**, *7*, 2770.
[47] Saalfrank, R. W.; Bernt, I.; Chowdhry, M. M.; Hampel, F.; Vaughan, G. B. M. *Chem. Eur. J.* **2001**, 2765.
[48] Kawa, M.; Fréchet, J. M. J. *Chem. Mater.* **1998**, *10*, 286.
[49] Fréchet, J. M. J. *Proc. Natl Acad. Sci. USA* **2002**, *99*, 4782.
[50] Saalfrank, R. W.; Deutscher, C.; Maid, H.; Ako, A. M.; Sperner, S.; Nakajima, T.; Bauer, W.; Hampel, F.; Heβ, B. A.; van Eikema Hommes, N. J. R.; Puchta, R.; Heinemann, F. W. *Chem. Eur. J.* **2004**, *10*, 1899.
[51] Saalfrank, R. W.; Deutscher, C.; Sperner, S.; Nakajima, T.; Ako, A. M.; Uller, E.; Hampel, F.; Heinemann, F. W. *Inorg. Chem.* **2004**, *43*, 4372.
[52] Beatty, A. M.; Granger, K. E.; Simpson, A. E. *Chem. Eur. J.* **2002**, *8*, 3254.
[53] Su, C.-J.; Cai, Y.-P.; Chen, C.-L.; Smith, M. D.; Kaim, W.; zur Loye, H.-C. *J. Am. Chem. Soc.* **2003**, *125*, 8595.
[54] Stoddart, J. F.; Fyfe, M. C. T. *Acc. Chem. Res.* **1997**, *30*, 393.
[55] Janiak, C. J. *J. Chem. Soc., Dalton Trans.* **2000**, 3885.
[56] Chang, C.-H.; Hwang, K. C.; Liu, C.-S.; Chi, Y.; Carty, A. J.; Scoles, L.; Peng, S.-M.; Lee, G.-H.; Reedijk, J. *Angew. Chem.* **2001**, *113*, 4787.
[57] *Angew. Chem., Int. Ed. Engl.* **2001**, *40*, 4651.
[58] Schmitt, W.; Baissa, E.; Mandel, A.; Anson, C. E.; Powell, A. K. *Angew. Chem.* **2001**, *113*, 3690.
[59] *Angew. Chem., Int. Ed. Engl.* **2001**, *40*, 3578.
[60] Xiong, R.-G.; You, X.-Z.; Abrahams, B. F.; Xue, Z.; Che, C.-M. *Angew. Chem.* **2001**, *113*, 4554.
[61] *Angew. Chem., Int. Ed. Engl.* **2001**, *40*, 4422.
[62] Ying, J. Y.; Melmert, C. P.; Wong, M. S. *Angew. Chem.* **1999**, *111*, 58.
[63] *Angew. Chem., Int. Ed. Engl.* **1999**, *38*, 56.
[64] Tsuzuki, S.; Honda, K.; Uchimura, T.; Mikami, M.; Tanabe, K. *J. Am. Chem. Soc.* **2002**, *124*, 104.
[65] Lehn, J.-M. *Science* **2002**, *295*, 2400.
[66] Lehn, J.-M. *Proc. Natl Acad. Sci. USA* **2002**, *99*, 4763.
[67] Shieh, D.-L.; Shiu, K.-B.; Lin, J.-L. *Eur. J. Inorg. Chem.* **2004**, 2223.
[68] Perrin, D. D.; Armarego, W. L. F. *Purification of Laboratory Chemicals*; Pergamon: Oxford, 1988.
[69] *SADABS* and *SHELXTL NT 6.12*, Bruker AXS Inc., Madison WI, USA, 2002.
[70] Lingenfelder, H. A.; Spillmann, H.; Dmitriev, A.; Stepanow, S.; Lin, N.; Barth, J. V.; Kern, K. *Chemistry* **2004**, *10*, 1913.
[71] Saalfrank, R. W.; Maid, H.; Hampel, F.; Peters, K. *Eur. J. Inorg. Chem.* **1999**, 1859.
[72] Hamers, R. J.; Tromp, R. M.; Demuth, J. E. *Phys. Rev. Lett.* **1986**, *56*, 1972.
[73] Novokmet, S.; Alam, M. S.; Dremov, V.; Heinemann, F. W.; Müller, P.; Alsfasser, R. *Angew. Chem.* **2005**, *117*, 813.
[74] *Angew. Chem., Int. Ed. Engl.* **2005**, *44*, 803.
[75] Rivera, M.; Williamson, R. L.; Miles, M. J. *J. Vac. Sci. Technol. B* **1996**, *14*, 1472.